Catalysis Letters Vol. 98, No. 4, December 2004 (© 2004)

Support effects in nerol hydrogenation over Pt/SiO₂, Pt/H-Y and Pt/H-MCM-41 catalysts

Päivi Mäki-Arvela[1], Narendra Kumar[1], Ivo Paseka[2], Tapio Salmi[1] and Dmitry Yu. Murzin[1,]*

[1]*Laboratory of Industrial Chemistry, Process Chemistry Centre, Åbo Akademi University, FIN-20500 Åba/ Turku, Finland* [2]*Institute of Inorganic Chemistry, Academy of Sciences of Czech Republic, Rez, Czech Republic*

Received 9 June 2004; accepted 10 September 2004

Chemoselective hydrogenation of nerol was investigated over Pt/SiO_2, Pt/H-Y and Pt/H-MCM-41 catalysts. The initial total reaction rates decreased in following order:Pt/H-Y > Pt/SiO_2 > Pt/H-MCM-41. Nerol hydrogenation was found to be an apparent structure sensitive reaction. The selectivities to citronellol at 30% conversion of nerol were 65%, 55% and 25% over Pt/SiO_2, Pt/H-MCM-41 and Pt/H-Y, respectively.

KEY WORDS: nerol, hydrogenation, kinetics, selectivity, Pt, H-MCM-41.

1. Introduction

Nerol is an unsaturated alcohol, widely applied in perfumery industry. Annually 6000 tonnes of nerol and another alcohol geraniol and their esters as well as a product of nerol hydrogenation, citronellol and its esters are used for the synthesis of rose odour compounds [1]. Heterogeneous catalytic hydrogenation of nerol (A) has been very scarcely investigated [2,3]. Not only industrially, but also scientifically it is an interesting molecule, because besides hydrogenation it can undergo isomerization to an unsaturated aldehyde, citronellal (B) (figure 1) [3], which can in principle further be hydrogenated to 3,7-dimethyloctanal (F). The main hydrogenation products are citronellol (C) and 3,7-dimethyloctanol (G). Additionally hydrocarbons can be formed by hydrogenolysis of nerol [3].

Citronellol is a valuable intermediate for the production of fragrances [1] and pheromones [4]. It can be synthesized by several methods, for instance catalytic hydrogenation starting from citral [5], citronellal [6,7], nerol [3] or geraniol [8], or hydrodealumination of the alumino-derivative of dihydromyrcene followed by oxidation and hydrolysis [9] or via treating an acyclic terpene with $NaBH_4$ and $AlCl_3$ with further hydration and oxidation with H_2O_2 [10]. Furthermore C can be prepared via pyrolysis of pinane followed by hydration [11]. In the catalytic hydrogenation selectivities of over 95% have been achieved in citral hydrogenation over Ni/Al_2O_3 catalyst in ethanol [5]. Over Rh black [12] and Ni/Cr_2O_3 [13] the maximum selectivities to C in citral hydrogenation of 95% and 80%, have been respectively achieved, however, under diffusion limitations. Citral hydrogenation was very selective to C over a bimetallic $NiMo_{12}$ catalyst in 2-propanol [14]. Citronellal has been hydrogenated to citronellol with the selectivities up to 90% over Ru/TiO_2 catalyst [6]. Very high selectivities for C (94%) have been reported in geraniol hydrogenation over pt/Y in toluene [8]. The only products were C and D. Hydrogenation of nerol over Pt/SiO_2 in hexane has been reported in literature [2]. The main product was citronellol. Additionally the formation of D (below 5%) was observed. However the full kinetic curves were not reported in [2]. The concentration-time dependences of nerol hydrogenation were presented for a copper chromite catalyst at 140 °C in decalin [3] with a maximal yield of around 25% in B. Citronellal reacted further to C with small amounts of hydrocarbons also observed in the product mixture. However, neither D nor G were formed. The maximum selectivity to C was about 68%.

Metal supported, mesoporous H-MCM-41 is a potential support material for chemoselective hydrogenations [8,15–18], because of its large specific surface area and larger pores than zeolites. MCM-41 has recently been used as support in the hydrogenation and cyclization of citral to menthols over Ni/Al-MCM-41 [15], geraniol over Pt/MCM-41 [8], cinnamaldehyde over Ru-MCM-41 [16,17] and prostaglandin intermediates over Ru-MCM-41 [18]. In geraniol hydrogenation at 80 °C and 20 bar in toluene over Pt/MCM-41 the selectivities to citronellol were high, 85%; the only other product was 3,7-dimethyloctanol [8]. The catalyst used in the work of Tas *et al.* [8] was prepared via impregnation of MCM-41 with $Pt(NH_3)Cl_2$. Surprisingly no hydrogenolysis products were observed in geraniol hydrogenation even over very acidic Pt/H-Y catalyst [8].

Despite the industrial application, the hydrogenation mechanism, kinetics as well as catalyst selection in nerol hydrogenation have been very scarcely addressed in the

---

*To whom correspondence should be addressed.
E-mail: dmurzin@abo.ji

1011-372X/04/1200–0173/0 © 2004 Plenum Publishing Corporation

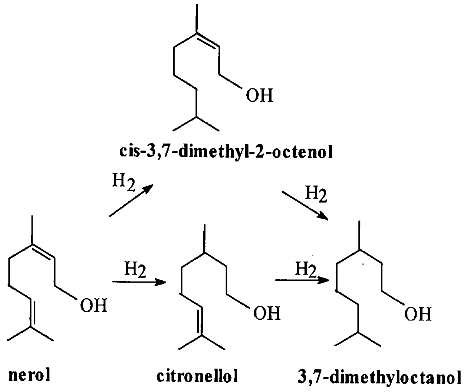

Figure 1. Simplified reaction scheme in nerol hydrogenation.

open literature [2,3]. To the best of our knowledge, only Hubaut [3] have reported the whole concentration-time curves for nerol hydrogenation, for a copper chromite catalyst. The aim of this work was to investigate chemoselective hydrogenation of nerol over Pt/H-MCM-41, Pt/H-Y and Pt/SiO_2 catalysts. These supports were selected also for the purpose of elucidating the influence of acidity and shape selectivity on catalytic performance.

2. Experimental

2.1. Catalyst preparation

The Na-MCM-41 mesoporous molecular sieve was synthesized at 100 °C from tetradecyltrimethylammonium bromide as a surfactant, sodium silicate solution (Merck) as a source of silica and sodium aluminate (Riedel Haen) as a source of alumina using the methods described in the literature [19,20]. The synthesized material was washed with distilled water, dried at 100 °C and calcined at 540 °C in order to remove the surfactant. H-MCM-41 was prepared from Na-MCM-41 via ionexchange with 1 M NH_4CI, followed by calcination at 530 °C.

The silica (Merck) and NH_4-Y (Zeolyst International, CBV 712), were obtained from commercial sources. The ammonium form of Y was calcined using a muffle oven. The H-Y and H-MCM-41 catalsyts were prepared by impregnating the support with H_2PtCl_6 (40%, Degussa) in a rotary evaporator (Buchi Rotavapor R114) for 24 h; Pt/SiO_2 catalyst was prepared using an incipient wetness method and the same Pt precursor. The impregnated catalysts were dried in an oven at 100 °C.

2.2. Catalyst characterization

The metal loadings of the catalysts prepared by the impregnation method were measured by DCP spectrometer (ARL-Fisons Instruments, USA).

The mean Pt crystallite size, phase purity and structure were investigated with XRD-diffractometer (philips PW 1800). The catalysts were reduced at 350 °C for 2 h in flowing hydrogen (AGA, 99.999%) prior to measuring the mean Pt crystallite sizes. The Sherrer equation was used in determining the mean crystallite sizes. Additionally the phase purity of zeolite supports was measured and compared with the XRD-pattern of the metal modified catalysts in order to eliminate the possibility of peaks coinciding with support patterns.

The concentration of Brønsted and Lewis acid sites in H-Y, H-MCM-41 and SiO_2 supports were determined by FTIR (ATI Mattson FTIR) with pyridine ($\geq$99.5%, a.r) as a probe molecule. The catalysts were pressed into thin wafers (10–12 mg/cm^2) and evacuated at 450 °C for 60 min after which the adsorption of pyridine was carried out at 100 °C for 30 min. The desorption of pyridine was carried out at 200 °C and spectra were recorded at 100 °C with a spectral resolution of 2 cm^{-1}. The quantification of adsorbed pyridine was based on the molar extinction coefficient for pyridine determined by Emeis [21]. The dry support weights were used in calculations.

The specific surface area of the catalysts was measured with nitrogen adsorption (Sorptometer 1900, Carlo Erba Instruments). The catalysts were outgassed at 200 °C for 4 h prior the measurements. The Dubinin method was used to determine the surface area of microporous Pt/H-Y, while the BET method was applied for Pt/SiO_2 and Pt/H-MCM-41.

The specific metal surface area was measured by using electrochemical voltammetric method [22]. The catalysts were sieved (mesh size 0.125 mm) and mixed with fine-powdered graphite in the ratio 1:1. The homogenization of the sample was carried out in a homogenizer (Janke Kunkel GMBH Type A10). In order to achieve good adherence of the sample to the electrode collector (Pt, mesh size 0.38 mm), water-diluted PTFE solution (Aldrich) was added and the suspension was dried to a constant weigh at 100 °C.

The formed gummy mass was spread onto a supporting gauze in a thin layer and pressed (5000 kg/cm^2). The weight of the prepared electrodes was about 15 mg. Electrochemical measurements were carried out in 1 M H_2SO_4.

The current response was detected in a digital form by AID converter (S 711 Advantech) and a PC computer. The integral charge, enclosed by the voltammetric curve in the potential region $E = 0.05 - 0.35$ V was acquired by the numerical integration. The value 210 μC/cm^2 was used for the evaluation of the platinum specific surface.

2.3. Catalyst testing

Hydrogenation of nerol (90%, Fluka 72170) was carried out in an autoclave (Autoclave Engineers, $V_L = 200$ ml) under kinetic region [23] by using the sieved catalyst particles (< 63μm) and the stirring rate of 1500 rpm in all experiments in order to avoid diffusion limitations. The catalyst was reduced at 350 °C for 2 h with flowing hydrogen (AGA, 99.999%) after which it was cooled to reaction temperature. The deoxygenated solvent, 2-pentanol (Fluka) and reactant were injected into the reactor after which the reaction mixture was heated up to the desired temperature. Hydrogen pressure and temperature were 10 bar and 70 °C, respectively. The initial nerol concentration was 0.01 M. Typically 200 mg of catalyst and 200 ml of solvent was used in the experiments. The molar ratio of nerol/Pt varied between 40 and 80 M. The samples were taken from the reactor and analyzed by a gas chromatograph equipped with a capillary column (HP-5, length 30 m, internal diameter 0.32 mm, film thickness 0.25μm). The injector and detector temperatures were 250 °C and 300 °C, respectively. The products were confirmed by GC-MS. All products were separated, except *trans*-3,7-dimethylocten-2-ol (E) and 3,7-dimethyloctanol (G), which co-eluated.

3. Results and discussion

3.1. Support characterization

The phase purity of H-Y, H-MORD and H-MCM-41 supports was investigated by XRD. All the samples exhibited highly phase pure materials of MORD, H-Beta and H-Y. The XRD-pattern of synthesized MCM-41 confirmed the presence of original pure hexagonal phase of MCM-41 as observed by Yu *et al.* [24].

Both Brønsted and Lewis acid site concentrations of the H-Y, H-MCM-41 and SiO_2 supports were determined with FTIR. The spectra of Beta zeolite and H-MCM-41 are shown in figure 2. The Brønsted acid concentration corresponded to the absorption band of pyridinium ion at 1545 cm^{-1}, whereas the Lewis acid site concentration is determined by the absorption band at 1452 cm^{-1}. The Brønsted acid site concentration is very high for H-Y, while lower Brønsted acidity was obtained for H-MCM-41 (table 1). Not surprisingly the silica exhibited no Brønsted acid sites. The concentration of Lewis acid sites decreased in the following order: H-MCM-41 > H-Y >> SiO_2.

Table 1
Concentration of the Brønsted and Lewis acid sites in different catalyst supports. Desorption of pyridine carried out at 200 °C

Catalyst	Brønsted acid sites (μmol/g cat.)	Lewis acid sites (μmol/g cat.)
H-MCM-41	89	168
H-Y	291	165
SiO_2	0	7

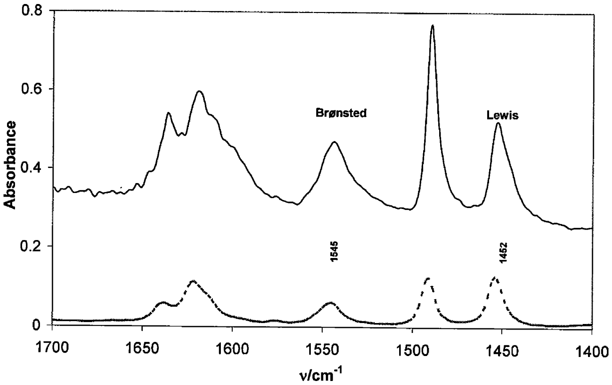

Figure 2. FTIR spectra of adsorbed pyridine on H-Beta and on H-MCM-41 catalysts. A solid line corresponds to H-Beta and a dashed line to H-MCM-41.

3.2. Catalyst characterization

The Pt loading and specific surface area of the catalysts are presented in table 2. The cyclic voltammetric curves for these catalysts are shown in figure 3. The metal loadings varied between 2.0 and 5.0 wt.%. The highest metal loading was in Pt/SiO_2, which was prepared by incipient wetness method. The specific surface areas of the catalysts were, as expected, largest for Pt/H-MCM-41 and Pt/H-Y. Additionally the specific surface areas of the spent catalysts used in nerol hydrogenation were measured. The specific surface area of Pt/SiO_2 was reduced only by 15% during nerol hydrogenation, whereas the decrease of specific surface area in the two other catalysts was much greater (table 2).

The mean Pt crystallite sizes were investigated by XRD. The patterns of Pt modified H-Y indicated that the original structure of zeolite remained intact. The mean Pt crystallite sizes of the catalysts determined by XRD are presented in table 3. The specific Pt surface areas determined by cyclic voltarnmetry (figure 3) decreased in the following order: Pt/H-Y > Pt/H-MCM-4l > Pt/SiO_2 (table 3). These values correlated well with the mean Pt crystallite sizes determined by XRD (table 3).

3.3. Hydrogenation of nerol

3.3.1. Initial hydrogenation rates over different catalysts

The initial reaction rates of nerol over the three catalysts in 2-pentanol are compared in table 4. These rates decreased in the following order: Pt/H-Y > Pt/

Table 2
The catalysts used in the hydrogenation of nerol

Catalyst	Specific surface area (m^2/g cat.)	Specific surface area of the spent catalyst (m^2/g cat.)	Pt loading (DCP) wt.%
Pt/H-MCM-41	1189	524	2.5
Pt/H-Y	1088	636	3.8
Pt/SiO_2	412	352	5.0

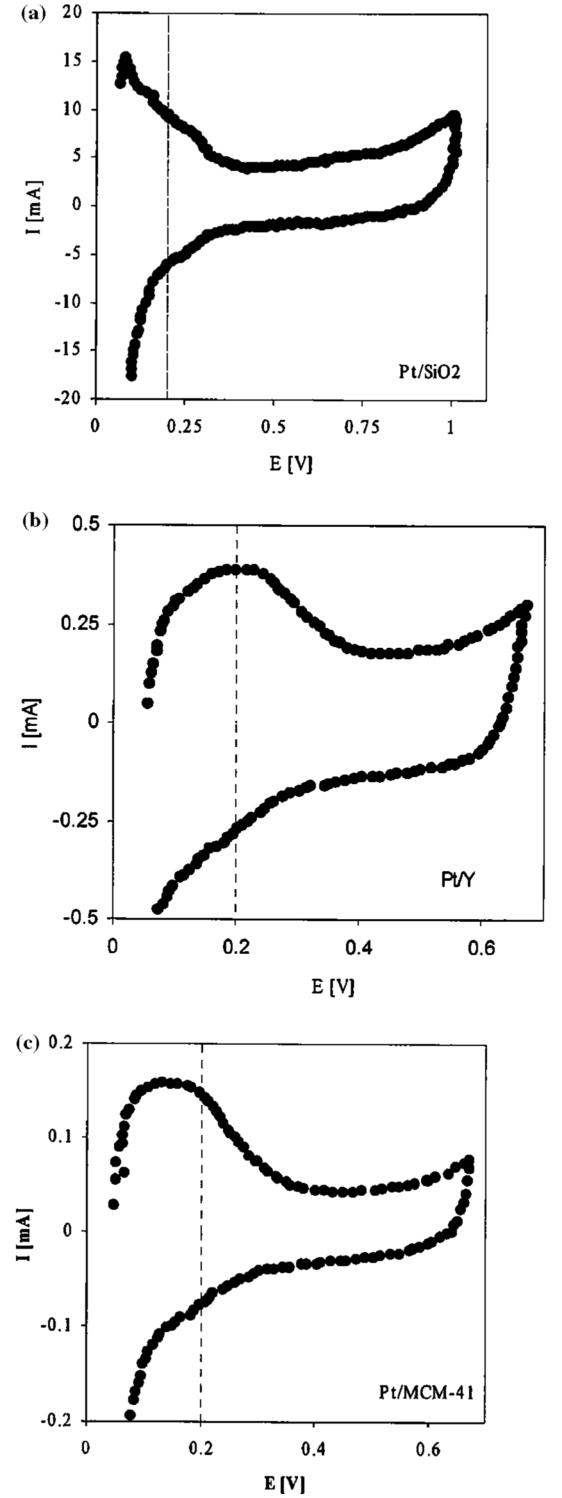

Figure 3. Cyclic voltammetric results from different catalysts: (a) Pt/SiO$_2$, (b) Pt/H-Y and (c) Pt/H-MCM-41.

SiO$_2$ > Pt/H-MCM-41. The highest reaction rate was achieved over Pt/H-Y, which exhibited the highest specific Pt surface area (table 3). When the initial hydrogenation rate and initial hydrogenolysis rate were separated, it turned out that the highest initial hydrogenation rate was obtained with Pt/SiO$_2$, whereas lower initial hydrogenation rates were achieved over Pt-H-MCM-41 and Pt/H-Y (table 4). The low TOF value over Pt/H-Y compared to Pt/SiO$_2$ can be explained by the catalyst deactivation (see next chapter). In spite of the fact that the mean Pt particle size measured by XRD was 3.5–3.7 nm for Pt/H-Y (table 3), the Pt particles in Pt/H- Y are locating both inside and outside the zeolite structure. This was confirmed by measuring the impact of Pt on zeolite acidity via pyridine adsorption with FTIR [26]. Furthermore XRD method gives the mean value of metal particle sizes including very large metal crystallites being catalytically inactive.The most active catalyst, PtlSiO$_2$, exhibited the smallest specific Pt surface area (table 3). The initial hydrogenolysis rate increased with increasing concentration of Brønsted acid sites in different supports (tables 1 and 4) and no hydrogenolysis products were observed over Pt/SiO$_2$ exhibiting no Brønsted acid sites. On the contrary hydrocarbons were formed in gas phase hydrogenation of allyl alcohol over Pt/SiO$_2$ catalyst [27], however this reaction was carried out in the gas phase and the stability of the low molecular allyl alcohol is lower than that of a longer alcohol, nerol. The catalytic activity of Pt/H-MCM-41 (table 4) was low given its small the mean Pt crystallite size (table 3). For structure insensitive reactions the TOF calculated by dividing the initial rate by the specific metal surface area should not depend on the metal loading (table 2). Although the TOF was clearly seen to be dependent on the metal crystallite particle size, we can only conclude that nerol hydrogenation over Pt supported catalysts is an apparent structure sensitive reaction. The reason for this apparent behavior is that prominent hydrogenolysis reaction over Pt/H-Y makes the direct comparison of the catalytic performance difficult, because over Pt/SiO$_2$ no hydrogenolysis reaction occurred.

Table 3
Specific Pt surface areas determined by cyclic voltammetry and mean Pt particle sizes measured by XRD

Catalyst	Specific surface area (m^2/g Pt)	Mean Pt particle size by XRD (nm)
Pt/H-MCM-41	67	3.1–4.1
Pt/H-Y	78	3.5–3.7
Pt/SiO$_2$	17	24

3.3.2. Conversions after prolonged reaction times

The conversion of nerol as a function of time over the three catalysts is presented in figure 4. Comparison of nerol conversion after 120 min reaction time shows that the amount of converted nerol calculated per gram Pt decreased in following order: Pt/H- Y > Pt/SiO$_2$ = Pt/H-MCM-41 (table 4).

The catalyst deactivation was additionally measured by recording the specific surface areas of the spent catalysts by nitrogen adsorption. The results indicated

Table 4
Catalyst screening in nerol hydrogenation

Catalyst	Initial total reaction rate (mmol/min/g Pt)	Initial hydrogenation rate (mmol/min/g Pt)	Initial hydrogenolysis rate (mmol/min/g Pt)	TOF (s^{-1})	Conversion (%)	Amount of converted A after 120 min (mmol/g Pt)	Selectivity to C (%)[a]	Yields of E and G at 40% conversion level (mmol/g Pt)	Yields by products at 40% conversion level (mmol/g Pt[b])
Pt/H-MCM-41	14	13.9	0.1	0.19	43	172	43	32	40
Pt/H-Y	45	19	26	0.51	100	263	25	20	66
Pt/SiO_2	25	25	0	1.30	86	172	65	22	0

Initial reaction rate, initial hydrogenation rate and initial hydrogenolysis rate of nerol (A), TOF, conversion after 2 h, selectivity to citronellol (C) and yields of trans-3,7-dimethyl-2-octenol (E) and 3,7-dimethyloctanol (G) (one peak in GC) and by-products over different catalysts. Conditions: 70 °C, 10 bar H_2, solvent 2-pentanol.

[a] at 40% conversion of nerol

[b] the major by-products were 3,7-dimethyl-2-octene and 3,7-dimethyloctane.

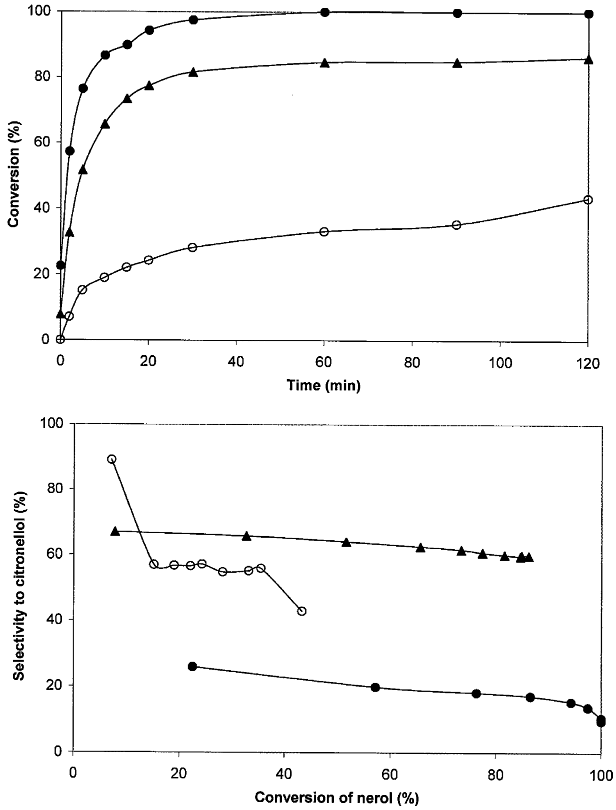

Figure 4. (a) Conversion of nerol and (b) selectivity to citronellol over different catalysts. Conditions: 70 °C, 10 bar, solvent 2-pentanol. Symbols: (○) Pt/H-MCM-41, (●) Pt/H-Y and (▲) Pt.SiO_2

that the specific surface area decreased about 56% for Pt/H-MCM-41 and 42% for Pt/H-Y catalyst, whereas the corresponding value for Pt/SiO_2 was about 15% indicating only minor accumulation of organic material in this catalyst. In spite of the prominent decrease in specific surface area of the spent Pt/H-Y, the total conversion of nerol was achieved within 60 min (figure 4). The pore blockage or land accumulation of organic material inside Pt/H-Y did not decrease dramatically the catalyst performance. This was not, however, the case in Pt/H-MCM-41, over which only 43% conversion of nerol was achieved within 120 min. The pore sizes in Pt/H-Y are three- to four-times smaller than in Pt/H-MCM-41 and thus a larger part of Pt particles is located inside the H-MCM-41 than inside H-Y, because the mean Pt particle sizes in these catalysts are close to each other (table 3). This could partially explain the lower catalytic activity of Pt/H-MCM-41 compared to Pt/H-Y.

Catalyst deactivation can generally originate from sintering, leaching, poisoning or cracking and coke formation. In nerol hydrogenation the catalyst deactivation is caused by coke formation due to the observed formation of hydrocarbons. Decarbonylation of unsaturated alcohols during catalytic hydrogenation is well documented in the literature [2]. Analogously to our results in the work of Singh *et al.* [2] a very fast catalyst (Pt/SiO_2) deactivation was observed in geraniol hydrogenation at 100 °C and 20 bar H_2.

3.3.3. Selectivity to citronellol

The highest selectivity to citronellol (around 65%) was obtained over Pt/SiO_2 around 65% (figure 4, table 4), whereas over two other catalysts the selectivities were lowered due to formation of hydrogenolysis products, 3,7-dimethyl-2-octene (H) and 3,7-dimethyloctane (I). The selectivity to citronellol was nearly independent of the nerol conversion over Pt/SiO_2 and over Pt/H-Y. The latter catalyst, however, promoted the undesired hydrogenolysis reactions and thus the selectivity to citronellol remained low, at 26%. Pt/SiO_2 catalyst was very selective for producing mainly hydrogenation products, whereas over mesoporous Pt/H-MCM-41 the selectivities to citronellol decreased over increasing nerol conversion due to consecutive hydrogenation and hydrogenolysis. The selectivity to citronellol was not given in [2], but over Cu/Cr_2O_4 a maximum selectivity to citronellol of 70% was achieved in decalin at 140 °C [3]. The formation of citronellal via isomerization of nerol was minor over all three catalysts (<3%). This is consistent with the work of Singh *et al.* [2], who observed negligible isomerization of nerol to citronellal. Hubaut [3], who used Cu/Cr_2O_4 catalyst, observed up to 25% yield of citronellal. The ratio between the yields of citronellol and *cis*-3,7-dimethyl-2-octenol varied in a range of 10–15 over all catalysts, indicating that it is easier to hydrogenate the double bond at the position C2 than at C7. Comparison of the yields of by-products and the yields of the sum of trans-3,7-dimethyl-2-octenol and 3,7- dimethyloctanol (one peak in GC) at 40% nerol conversion indicated that the amount of hydrogenolysis products formed per gram of Pt was quite low over Pt/SiO_2, whereas over the other catalysts the normalized yields of by-products were more than 40 mmol/g Pt (table 4). Additionally the yield of hydrogenolysis products correlated with the concentration of Brønsted acid sites of the support, but not with the concentration of Lewis acid site. Recent reports in the literature [15,25] have suggested the possibility of citronellal cyclisation to isopulegol, with further hydrogenation to menthol over Ni and Ir supported on MCM-41. No cyclisation products were noticed in the present study.

4. Conclusions

Liquid phase hydrogenation of nerol was studied over Pt supported on wide porous silica, microporous zeolite Y and mesoporous MCM-41.

The highest total reaction rates were observed over Pt/H-Y catalyst followed by Pt/SiO_2 and Pt/H-MCM-41. The mesoporous Pt/H-MCM-41 catalyst exhibited very low catalytic activity compared to Pt/H-Y, although their mean Pt surface area determined by cyclic voltammetry, were about the same. The catalyst deactivation was especially severe in case of Pt/H-MCM-41. The lower catalytic activity and lower final conversion of nerol after 120 min over this catalyst is partially explained by pore blocking, thus preventing access to Pt particles located inside H-MCM-41 structure. Due to smaller size of pores in Y -zeolite Pt particles are located preferentially outside. Therefore substantial decrease of the specific surface area in the spent catalyst was not accompanied by as strong a deactivation as was seen for Pt/H-MCM-41. By comparing the initial hydrogenation and hydrogenolysis rates, it could be inferred that the hydrogenation of nerol is an apparent structure sensitive reaction.

The most selective catalyst for production of citronellol was Pt/SiO_2, with a selectivity of about 65%. The selectivity to citronellol did not depend on the nerol conversion over Pt/SiO_2 and over Pt/H-Y, whereas over Pt/H-MCM-41 it decreased with increasing conversion due to hydrogenolysis of nerol. However the highest selectivity over Pt/H-Y remained low at 26% due to hydrogenolysis and consecutive hydrogenation reactions. The amount of hydrogenolysis products correlated with the concentration of Brønsted acid sites. The ratio between the yields of parallel hydrogenation products, e.g. citronellol and *cis*-3,7- dimethyl-2-octenol, was about 10–15 for all three catalysts indicating that it is easier to hydrogenate the double bond at C2 than at C7. The yields of isomerization products, citronellal and 3,7-dimethyloctanal were very minor over all three catalysts.

Acknowledgments

This work is part of the activities at the Åbo Akademi Process Chemistry Centre within the Finnish Centre of Excellence Programme (2000–2005) by the Academy of Finland. Authors are grateful to Mr. Markku Reunanen (Åba Akademi) for the MS analysis and to Mr. Teemu Heikkilä, University of Turku for XRD measurements.

References

[1] D. Pybus and C. Sell (eds), The chemistry of fragrances, (The Royal Society of Chemistry, Cambridge, UK, 1999), p. 54.

[2] U.K. Singh, M.N. Sysak and M.A. Vannice, J. Catal. 191 (2000) 181.

[3] R. Hubaut, React. Kinet. Catal. Lett. 46 (1992) 25.

[4] P.H.G. Zarbin, A. Reckziegel, E. Plass, A.R.M. de Oliveira, F. Simonelli and F.de A. Marques, J. Braz., Chern. Soc. 11 (2000) 572.

[5] P. Mäki-Arvela, L.-P. Tiainen, M. Lindblad, K. Demirkan, N. Kumar, R. Sjöholm, T. Ollonqvist, J. Väyrynen, T. Salmi and D.Yu. Murzin, Appl. Catal. A: Gen. 241 (2003) 271.

[6] A.A. Wismeijer, A.P.G. Kieboom and H. van Bekkum, Appl. Catal. 25 (1986) 181.

[7] H.-G. Goebbel, T. Gerlach, G. Wegner, H. Fuchs, S. Unterverricht and A. Salden, WO 2004007411 (2004) .

[8] D. Tas, R.F. Parton, K. Vercruysse and P.A. Jacobs Stud. Surf. Sci. Catal., H. Chon, S.-K. Ibm and Y.S. Uh (eds.) Vol. 105, (Elsevier, Amsterdam, 1997) 1261 p.

[9] V.V. Goidin, V.V. Molchanov, R.A. Buyanov, G.A. Tolstikov and A.I. Lukashevich, RU 2196762 (2003).

[10] E.L. Woroch, I. Cole and J.W. Cole, US 2990422, (1961).

[11] S.A. Voitkevich, N.N. Zelenetskii, V.V. Kashnikov and O.N. Zhuchkova, Maslozhirovaya Promyshlennost 2 (1975) 28.

[12] A. Pak, D. Sokolskii and S. Konuspaev, Kinet. Katal. 21 (1979) 670.

[13] D. Sokolskii, A. Pak and S. Konuspaev, Kinet. Katal. 20 (1979) 884.

[14] J. Court, J. Jablonski and S. Hamar-Thibault , Stud. Surf. Sci. Catal. , M. Guisnet, J. Barbier, J. Barrault, C. Bouchoule, D. Duprez, G. Pérot and C. Montasssier (eds) Vol. 78 (Elsevier, Amsterdam, 1993) 155 p.

[15] A.F. Trasarti, A.J. Marchi and C.R. Apesteguía, J. Catal. 224 (2004) 484.

[16] J. Hajék, N. Kumar, P. Mäki-Arvela, T. Salmi, D.Yu. Murzin, I. Paseka, T. Heikkilä, E. Laine, P. Laukkanen and J. Väyrynen, Appl. Catal. A: Gen. 251 (2003) 385.

[17] N. Kumar, P. Mäki-Arvela, J. Hajék, T. Salmi, D.Yu. Murzin, T. Heikkilä, E. Laine, P. Laukkanen and J. Väyrynen, Microp. Mesop. Mater. 69 (3) (2004) 173.

[18] S. Coman, M. Florea, F. Cacti, V.I. Parvalescu, P.A. Jacobs, C. Danumah and S. Kaliaguine, Chem. Commun. 21 (1999) 2175.

[19] N. Kumar, F. Klingstedt and L.-E. Lindfors, Stud. Surf. Sci. Catal. A. Carma, F.V. Melo, S. Mendioroz and J.L.G. Fierro (eds) Vol. 130 (Elsevier, Amsterdam, 2000), 2981 p.

[20] J.S. Beck, US Patent 5057296 (1991).

[21] C.A. Emeis, J. Catal. 141 (1993) 347.

[22] K. Kinoshita and P. Stonehart, Modern Aspects of Electrochemistry, J.O.M. Bockris and B.E. Conway (eds) (Plenum Press, New York, 1977).

[23] R.A. van Santen, P.W. van Leeuwen, J.A. Moulijn and P.A. Averlill (eds) Stud. Surf. Sci. Catal. 2nd ed., Vol. 123, (Elsevier, Amsterdam, 1999) 375 p.

[24] J.S. Yu, J.Y. Kim and L. Kevan, Microporous Mater. 40 (2000) 135.

[25] F. Iosif, S. Coman, V. Pârvulescu, P. Grange, S. Delsarte, D. De Vos and P. Jacobs, Chem. Comm., 11 (2004) 1292.

[26] D. Kubicka, N. Kumar, P. Mäki-Arvela, M. Tiitta, V. Niemi, H. Karhu, T. Salmi and D.Yu. Murzin, J. Catal. (in press).

[27] C. Hoang-Van and O. Zegaoui, Appl. Catal., A: Gen. 164 (1997) 91.